Published in final edited form as:
Immunity. 2010 November 24; 33(5): 723–735. doi:10.1016/j.immuni.2010.11.013.

Mzb1 Protein Regulates Calcium Homeostasis, Antibody Secretion, and Integrin Activation in Innate-like B Cells

Henrik Flach[1], **Marc Rosenbaum**[1], **Marlena Duchniewicz**[1], **Sola Kim**[2], **Shenyuan L. Zhang**[3], **Michael D. Cahalan**[3], **Gerhard Mittler**[1], and **Rudolf Grosschedl**[1,*]

[1]Department of Cellular and Molecular Immunology, Max Planck Institute of Immunobiology, Stuebeweg 51, 79108 Freiburg, Germany

[2]Gene Center, Department of Chemistry and Biochemistry, Ludwig-Maximilians University, 81377 Munich, Germany

[3]Department of Physiology and Biophysics, Institute for Immunology, University of California, Irvine, CA 92697, USA

SUMMARY

Marginal zone (MZ) B cells of the spleen and B1 cells, termed innate-like B cells, differ from follicular B cells by their attenuated Ca^{2+} mobilization, fast antibody secretion, and increased cell adhesion. We identified and characterized Mzb1 as an endoplasmic reticulum-localized and B cell-specific protein that was most abundantly expressed in MZ B and B1 cells. Knockdown of Mzb1 in MZ B cells increased Ca^{2+} mobilization and nuclear NFAT transcription factor localization, but reduced lipopolysaccharide-induced antibody secretion and integrin-mediated cell adhesion. Conversely, ectopic expression of an *Lck-Mzb1* transgene in peripheral T cells resulted in attenuated Ca^{2+} mobilization and augmented integrin-mediated cell adhesion. In addition to its interaction with the substrate-specific chaperone Grp94, Mzb1 augmented the function of the oxidoreductase ERp57 in favoring the expression of integrins in their activated conformation. Thus, Mzb1 helps to diversify peripheral B cell functions by regulating Ca^{2+} stores, antibody secretion, and integrin activation.

INTRODUCTION

Peripheral B lymphocytes consist of multiple cell populations that differ in their phenotype, functional properties, and anatomic locations (Allman and Pillai, 2008; Hardy et al., 2007; Martin and Kearney, 2000). In addition to the vast majority of conventional B cells, also termed follicular B (FoB) cells, which reside in lymph nodes and in the follicles of the spleen, marginal zone (MZ) B cells occupy the marginal sinus of the spleen, and B1 cells are predominantly found in the peritoneal and pleural cavities. MZ B and B1 cells have been termed “innate-like B cells,” given that these cells can be stimulated by ligands of Toll-like receptors (TLRs) to quickly differentiate into antibody-secreting cells that produce “natural,” polyreactive antibodies (Martin and Kearney, 2000; Rubtsov et al., 2008). Follicular B cells, in contrast, produce specific antibodies with much slower kinetics and require stimulation by both B cell receptor (BCR) and TLR for differentiation into antibody-

*Correspondence: grosschedl@immunbio.mpg.de.

SUPPLEMENTAL INFORMATION

Supplemental Information includes Supplemental Experimental Procedures, seven figures and two tables, and can be found with this article online at doi:10.1016/j.immuni.2010.11.013.

secreting cells (Richards et al., 2008). Murine marginal zone B cells have been shown to require weak BCR signals, whereas strong BCR signaling has been associated with follicular B cell development (Casola et al., 2004; Pillai and Cariappa, 2009). B1 cells also differ from follicular B cells in altered Ca^{2+} signaling and cell proliferation (Chumley et al., 2002). In particular, B1 cells display a reduced Ca^{2+} mobilization and exist in an "anergic" state in which they are less responsive to BCR stimulation (Dal Porto et al., 2004; Wong et al., 2002).

Another distinguishing hallmark of MZ B cells is the abundant expression of integrins, which helps the anchoring of these cells to the marginal zone of the spleen (Lu and Cyster, 2002). Integrins are cell-surface receptors composed of alpha- and beta-chain heterodimers that regulate cell adhesion and cell migration through bidirectional signaling (Hynes, 2002; Luo et al., 2007; Moser et al., 2009). Regulation of integrin-mediated cell adhesion depends on conformational changes of integrins, whereby three distinct states have been defined (Hynes, 2002; Luo et al., 2007). A bent conformation represents a low-affinity state, in which integrins have 1/500 and 1/10,000 the affinity for ligand binding compared to the extended-closed and extended-open conformations, respectively (Luo et al., 2007). Integrin conformations have been proposed to depend on long-range disulfide bonds in the β subunits, and mutations that introduce disulfide bonds to lock the conformation in the extended or bent states have been found to alter ligand binding affinity (Lu and Cyster, 2002; Luo et al., 2007).

MZ B cells and B1 cells also differ from FoB cells by their fast kinetics of antibody secretion in response to lipopolysaccharide (LPS) stimulation, and B1 cells have been reported to secrete antibodies spontaneously (Rubtsov et al., 2008). All these processes depend on functions of the endoplasmic reticulum (ER), which acts as a major intracellular calcium store and provides a strongly oxidizing environment that facilitates disulfide bond formation and folding of complex glycoproteins, such as immunoglobulins and integrins (Cahalan, 2009; Todd et al., 2008; Tu and Weissman, 2004). A family of ER oxidoreductases, including protein disulfide isomerase (PDI) and ERp57 (PDIA3), allows for the efficient folding of glycoproteins by catalyzing the formation and isomerization of intra- and intermolecular disulfide bonds (Ellgaard and Ruddock, 2005). Oxidative protein folding of complex proteins in the ER also depends on chaperones. In particular, ERp57 forms a complex with calnexin and calreticulin, whereby these lectin chaperones mediate substrate recognition. The abundant chaperone BiP (Grp78) is found in a complex with other ER chaperones, such as Grp94 (gp96, Hsp90b1) and PDI (Ni and Lee, 2007). Grp94 has a limited substrate specificity, which includes integrins, TLRs and immunoglobulins, and conditional inactivation of Grp94 in B lymphocytes diminished surface expression of TLR and attenuated secretion of antibodies upon TLR stimulation (Liu and Li, 2008; Melnick et al., 1994; Randow and Seed, 2001). Given the multiple phenotypic differences between peripheral B cell subsets, the question arises as to which genes regulate the characteristic properties of innate-like B cells. Here, we show that Mzb1, an ER protein that is abundantly expressed in marginal zone B and B1 cells, regulates calcium signaling, integrin-mediated adhesion, and antibody secretion by interacting with ERp57 and forming a substrate-specific complex with the BiP and Grp94 chaperones. Thus, Mzb1 may help to diversify the functions of peripheral B cell subsets.

RESULTS

Mzb1 Regulates Cell Proliferation and BCR Responsiveness

To identify genes that are differentially expressed in peripheral B cell subsets, we screened cDNA clones of a pre-B cell minus erythroid subtractive cDNA library (Travis et al., 1991) for their expression in FoB cells, MZ B cells, and B1 cells. One clone, termed *Mzb1*, was

found to be expressed in MZ B and B1 cells at a substantially higher amount than in FoB cells. We confirmed the differential expression of Mzb1 by both immunoblot analysis with an Mzb1 monoclonal antibody and by quantitative RT-PCR (Figure 1A and Figure S1A available online). By RNA blot analysis, abundant *Mzb1* transcripts could be detected in all transformed B cell lines examined, regardless of their stage of differentiation (Figure S1B). Analysis of the tissue distribution of *Mzb1* transcripts indicated that the *Mzb1* gene is expressed predominantly in the spleen and lymph nodes (Figure S1C). *Mzb1* transcripts found in the thymus and lung could be accounted for by contaminating B cells, given that immunoglobulin κ transcripts were also detected. *Mzb1* cDNA contains an open reading frame of 188 amino acids (aa) with marked conservation from human to the chordate *Ciona* (Figure S1D). Mzb1 protein includes a CXXC thioredoxin motif at position 49, a potential amino-terminal signal sequence and a carboxy-terminal ER-retrieval sequence. We examined the processing of Mzb1 protein by mass-spectometric analysis and found protein cleavages after amino acids 18 and 20 (Figure S1D and Table S1). Two recent reports independently described the cloning of *Mzb1* as an ER protein, termed pERp1, which associates with IgM in plasmacytoma cells (Shimizu et al., 2009; van Anken et al., 2009). However, no activity was ascribed to pERp1, other than an observed 50% decrease in antibody secretion after knockdown in plasmacytoma cells.

We determined the subcellular localization of Mzb1 by fractionation of K46 B cells and immunohistochemical analysis of MZ B cells and NIH 3T3 cells stably transfected with an *Mzb1-GFP* gene construct (Figure 1B and Figures S1E and S1F). In transfected NIH 3T3 cells, the Mzb1-GFP fusion protein, but not a fusion protein lacking the N-terminal signal sequence, colocalized with the ER marker Bap31. Moreover, in the microsomal fraction of K46 B cells, the endogenous Mzb1 showed a similar resistance to proteinase-K treatment as the luminal ER protein BiP, and both proteins were efficiently digested by proteinase-K in the presence of the detergent Triton X-100 (Figure 1B). Thus, Mzb1 appears to be localized in the ER lumen.

To gain insight into the function of Mzb1, we generated stably transfected K46 B cell clones in which the expression of Mzb1 was markedly downregulated by an Mzb1-specific siRNA. As controls for the specificity of the siRNA-mediated knockdown, we used both cells carrying a nonspecific siRNA construct and Mzb1-knockdown cells retransfected with an siRNA-resistant (Mzb1*) expression construct. Immunoblot analysis with Mzb1 antibody revealed a marked reduction of protein expression in three independent Mzb1-knockdown clones and an efficient rescue of Mzb1 protein expression in knockdown cells retransfected with the siRNA-resistant Mzb1* construct (Figure 1C). The Mzb1-knockdown cells grew more quickly than the control-knockdown and Mzb1*-rescue cells (Figure 1E). By determining [H^3]-thymidine incorporation, we found that the unstimulated Mzb1-knockdown clones incorporated 4- to 6-fold more thymidine than control-knockdown cells (Figure 1D). No marked differences in the apoptosis of untreated or tunicamycin-treated Mzb1- and control-knockdown K46 cells were observed (Figure S1G). BCR stimulation resulted in similar thymidine incorporation in Mzb1- and control-knockdown cells, suggesting that Mzb1 may curb the proliferation of K46 B cells (Figure 1D). To examine whether Mzb1-knockdown results in activation of K46 cells similar to stimulation by BCR signaling, we analyzed tyrosine phosphorylation. Immunoblot analysis of lysates prepared from serum-deprived control-knockdown, Mzb1-knockdown, and Mzb1*-rescue cells demonstrated that tyrosine phosphorylation is enhanced in unstimulated Mzb1-knockdown cells and resembles the pattern observed with BCR-stimulated control-knockdown cells (Figure 1F). In this experiment, the stimulation of the BCR further increased tyrosine phosphorylation, suggesting that Mzb1 may be involved in setting a threshold for BCR-mediated signaling.

We also examined the effect of Mzb1 downregulation and Mzb1 overexpression on the proliferation of sorted FoB and MZ B cells by transduction of primary cells with bicistronic retroviruses expressing GFP and Mzb1-specific siRNA or GFP and Mzb1. To allow for retroviral transduction of FoB cells, we used anti-CD23, which stimulates them by inducing Ca^{2+} mobilization (Kolb et al., 1990). Consistent with anti-CD23-induced Ca^{2+} mobilization, NFAT2 was detected in the nucleus and cytosol of these cells (Figure S1H). In contrast, FoB cells purified by a different scheme, involving depletion of other B cell types with anti-CD9 (Won and Kearney, 2002), showed a predominant cytosolic localization of NFAT2 (Figure S1I). Anti-CD23-stimulated and transduced GFP-positive cells were sorted and analyzed for Mzb1 expression and cell proliferation (Figures 1G and 1H and Figure S1J). The transduced lymphocytes kept their surface phenotype (data not shown). In both MZ B and FoB cells, the downregulation of Mzb1 increased cell proliferation, whereas Mzb1 overexpression decreased proliferation. Consistent with the more abundant Mzb1 expression in MZ B versus FoB cells, the effects of Mzb1 downregulation were more pronounced in MZ B cells and those of Mzb1 overexpression were stronger in FoB cells (Figure 1H). Thus, the downregulation of Mzb1 increased cell proliferation and overall tyrosine phosphorylation, whereas Mzb1 overexpression decreased the proliferation rate.

Mzb1 Regulates Ca^{2+} Store Content and Ca^{2+} Signaling

Ca^{2+} is a second messenger that regulates multiple processes in immune cells (Vig and Kinet, 2009). In unstimulated cells, a low cytosolic Ca^{2+} concentration is maintained by sarcoplasmic-endoplasmic reticulum calcium ATPase (SERCA)-mediated pumping of Ca^{2+} into the ER and by the inactive states of Ca^{2+} channels. In stimulated cells, Ca^{2+} release from the ER stores results in Ca^{2+} influx and nuclear translocation of the Ca^{2+}-responsive transcription factor NFAT (Cahalan, 2009; Crabtree and Olson, 2002). To examine Ca^{2+} signaling in response to BCR stimulation, we measured the changes in free intracellular Ca^{2+} by flow cytometry. We observed an increase in stimulated Ca^{2+} concentrations relative to control-knockdown and rescue cells in all of the three analyzed clones of Mzb1-knockdown K46 B cells (Figures 2A and S2A). Complementation of Mzb1-knockdown cells with gene constructs expressing siRNA-resistant Mzb1* or Mzb1^{*CXXA} with a mutated CXXA motif resulted in similar attenuation of Ca^{2+} signaling (Figures 1C and 2A), suggesting that the function of Mzb1 is independent of its thioredoxin motif.

We confirmed the enhancement of Ca^{2+} signaling in Mzb1-knockdown cells by determining the real-time changes in free Ca^{2+} of individual cells (Figure 2B). The altered Ca^{2+} flux in BCR-stimulated Mzb1-knockdown cells could be a consequence of changes in the ER Ca^{2+} store content, an impaired Ca^{2+} influx from the cellular environment, or a defect in the BCR signaling pathway. Because Mzb1 is an ER resident, we measured potential changes in BCR-independent store-operated Ca^{2+} entry by treating cells with thapsigargin, an inhibitor of the SERCA pump. Thapsigargin treatment of Mzb1-knockdown and control K46 cells followed by the addition of extracellular Ca^{2+} showed that Mzb1 downregulation augmented ER Ca^{2+} depletion and increased Ca^{2+} influx (Figure 2C). Treatment of cells with the ionophore ionomycin in the absence of extracellular Ca^{2+} resulted in an increased Ca^{2+} flux in Mzb1-knockdown cells relative to control and rescue cells, suggesting that Mzb1 regulates the ER Ca^{2+} store, rather than store-operated Ca^{2+} entry (Figure S2B). Chemokine signaling also induces Ca^{2+} fluxes (Muller and Lipp, 2001); however, the effect of the Mzb1-knockdown on Ca^{2+} mobilization was unaffected by exposure to the chemokine CXCL13 prior to triggering of Ca^{2+} fluxes (Figures S2C and S2E). Thus, the effect of Mzb1 on Ca^{2+} mobilization appears to be independent of CXCR5 signaling.

As additional readout of altered Ca^{2+} fluxes, we analyzed the effects of Mzb1 downregulation or overexpression on the nuclear localization and/or activity of the Ca^{2+}-regulated NFATc transcription factors (Crabtree and Olson, 2002). In K46 B cells, which

normally have low NFAT activation, Mzb1 downregulation resulted in enhanced DNA binding by NFAT in electrophoretic mobility shift assays (Figure S2F) and activation of a luciferase reporter construct containing multimerized NFAT-binding sites (Figure S2G). In primary MZ B and B1 cells, Mzb1 downregulation enhanced nuclear localization of NFAT2 (NFATc1) relative to control siRNA-transduced cells (Figures 2D and 2E and Figure S2H). Conversely, overexpression of Mzb1 in FoB cells increased cytosolic localization of NFAT2 (Figures 2E and 2F), consistent with the reduction of BCR-mediated Ca^{2+} mobilization in Mzb1-overexpressing FoB cells (Figure 2G). Similarly, a reduced Ca^{2+} store content, released by ionomycin treatment, was observed in individual NIH 3T3 fibroblastic cells stably expressing Mzb1 (Figure 2H).

Finally, we directly measured the Ca^{2+} store content in individual Mzb1-expressing and control NIH 3T3 cells by measuring the fluorescence lifetime of a transiently transfected ER-localized cameleon Ca^{2+} indicator (Figures 2I and 2J; Luik et al., 2008). Mzb1-expressing NIH 3T3 cells showed a significant decrease in the Ca^{2+} store content relative to mock-transfected NIH 3T3 cells. Thus, the down- and upregulation of Mzb1 in primary MZ B and FoB cells result in opposite effects on experimentally induced Ca^{2+} fluxes and activation of the Ca^{2+}-responsive NFAT transcription factors. Taken together, these data indicate that Mzb1 regulates Ca^{2+} signaling via modulating the ER Ca^{2+} store content.

Proteomic Analysis of Mzb1-Associated Proteins

To identify potential Mzb1 interaction partners, we performed a gel filtration experiment with the microsomal fraction of K46 B cells. Immunoblot analysis of individual fractions indicated that the majority of Mzb1 is found in fractions corresponding to 25 kDa, whereas a small amount of Mzb1 was detected in higher molecular weight fractions of ~220 kDa (Figure 3A). The higher molecular weight complex of Mzb1 was sensitive to changes in Ca^{2+} concentration, given that its abundance was decreased by the addition of 2.5 mM Ca^{2+}. We crosslinked proteins in vivo to stabilize interactions prior to cell lysis and purified the Mzb1-associated proteins by precipitation with anti-Mzb1. The immunoprecipitates were separated by SDS-PAGE, and gel regions corresponding to Mzb1-specific bands were isolated from the anti-Mzb1 and the anti-EBNA isotype control lanes (Figure 3B). Mass spectrometry of the eluted proteins allowed for the identification of the chaperones Grp94 and BiP, as well as the protein disulfide isomerases ERp57 and PDIA6 (CaBP1) as Mzb1-associated proteins (Figure 3B and Table S2). In the anti-Mzb1 lane, we also detected a lower abundance of peptides derived from SERCA2b, a client protein of ERp57 (Li and Camacho, 2004), and integrin β1, a client protein of ERp57 and Grp94 (Yang and Li, 2005).

To confirm the associations of Mzb1 with the identified protein partners, we coimmunoprecipitated Mzb1 protein complexes from K46 B cell extracts in the absence and presence of Ca^{2+}. Both Grp94, a protein with high-affinity binding sites for Ca^{2+}, and ERp57 interact with their client proteins at high Ca^{2+} concentrations (Biswas et al., 2007; Li and Camacho, 2004). However, Grp94, ERp57, and BiP were efficiently coimmunoprecipitated with anti-Mzb1 in the absence of Ca^{2+} and less efficiently in the presence of 2.5 mM Ca^{2+}, suggesting that these proteins associate with Mzb1 in a calcium-dependent manner (Figures 3C and 3D). These interactions were also detected by coimunoprecipitations with antibodies against ERp57 and Grp94 (Figures S3A and S3B). Moreover, reprobing the immunoblot of the gel filtration experiments described above revealed an overlap of the ~220 kDa Mzb1 complex with ERp57 at low but not high Ca^{2+} concentrations (Figure 3A). In GST pull-down assays, recombinant Mzb1 interacted with both GST-BiP and GST-ERp57, but not with GST alone (Figure 3E). Addition of 10 mM DTT to a K46 cell lysate impaired coimmunoprecipitation of ERp57 and Mzb1, but not that of Grp94 and Mzb1, suggesting that the association of Mzb1 and ERp57 involves disulfide bonds (Figure 3F). Finally, we analyzed whether the association of Mzb1 with ERp57

competes for the interaction of ERp57 with calnexin and calreticulin. In coimmunoprecipitations with anti-ERp57, we detected abundant amounts of calnexin and calreticulin in lysates from siMzb1-knockdown cells, but not in lysates from control-knockdown and Mzb1*-rescue cells. Conversely, we observed coimmunoprecipitation of both Mzb1 and Grp94 in lysates from control-knockdown and Mzb1*-rescue cells (Figure 3G). These data suggest that the interaction of Mzb1 with ERp57 results in an exchange of ERp57-associated chaperones.

Mzb1 Regulates Antibody Secretion in LPS-Stimulated MZ B Cells

MZ B cells differ from FoB cells by their fast kinetics of antibody secretion, and therefore we examined whether Mzb1 downregulation or Mzb1 overexpression in sorted MZ B and FoB cells alters LPS-induced antibody secretion. ELISpot analysis of Mzb1 siRNA-expressing MZ B cells showed ~1/7 the number of ASCs relative to control siRNA-expressing MZ B cells (Figure 4A). Conversely, retroviral Mzb1 overexpression in FoB cells stimulated with anti-CD23 and suboptimal concentrations of LPS resulted in a 5-fold increase in the number of ASCs relative to mock-transduced cells. Moreover, overexpression of Mzb1 in MZ B cells increased the number of ASCs, whereas the downregulation of Mzb1 in FoB cells decreased the frequency of ASCs (Figure 4B). In ELISA assays, we detected an ~50% decrease of IgM secretion in Mzb1-knockdown MZ B cells and a two-fold increase in Mzb1-overexpressing FoB cells, relative to control cells (Figure S4). Flow cytometry analysis to detect CD138, a marker of ASCs (Tumang et al., 2005), indicated that only a minor fraction of LPS-stimulated and GFP-positive cells differentiated to CD138-positive cells (Figure 4C).

The function of TLR4, which transduces LPS signals, is altered in Grp94-deficient cells (Randow and Seed, 2001), and therefore we examined the surface expression of TLR4 and the transcriptional response to LPS. Mzb1-knockdown cells contain modestly reduced numbers of TLR4 molecules on the cell surface (Figure 4D). Quantitative RT-PCR analysis of MZ B cells transduced with Mzb1- or control-siRNA revealed reduced amounts of both uninduced and induced transcription of the NF-κB-regulated genes *Ccl22* and *Bcl2a1a* (encoding A1) in Mzb1-knockdown cells (Figure 4E; Genestier et al., 2007; Ghadially et al., 2005). As a control, transcription of the *Bcl2l1* (encoding Bcl-xL) gene was not affected. Therefore, Mzb1 regulates the secretion of antibodies in LPS-stimulated MZ B cells, but not the transcriptional response to LPS stimulation.

Mzb1 Regulates Cell Motility and the Activation of Integrins

A hallmark of MZ B cells is the abundant surface expression of αLβ2 (LFA-1), α4β7, and α4β1 (VLA-4) integrins, which allow for their sessile, non-recirculatory state (Lu and Cyster, 2002). Moreover, these integrins are regulated by chemokine-mediated, inside-out signaling (Kinashi, 2005). Static adhesion assays indicated that unstimulated control siRNA-transduced MZ B cells displayed moderate adhesion to the LFA-1 ligand ICAM-1 and the VLA-4 ligand VCAM-1, which could be markedly increased by treatment of cells with the chemokines CXCL13 or CXCL12. In Mzb1-knockdown MZ B cells, we observed a pronounced decrease in adhesion to ICAM-1 and VCAM-1 in the absence of chemokines, which was further enhanced by the addition of CXCL12 or CXCL13 (Figure 5A). This decrease in integrin-mediated adhesion in Mzb1-knockdown MZ B cells was confirmed by the reduced ability of these cells to bind soluble ICAM-1 or VCAM-1, as determined by flow cytometry (Figures 5B and 5C; Sebzda et al., 2002).

Finally, we examined the functional status of LFA-1 and VLA-4 on Mzb1-knockdown MZ B cells by analyzing their chemotactic response to CXCL13 on transwell filters coated with ICAM-1 or VCAM-1 (Ansel et al., 2002; Lu and Cyster, 2002). In Mzb1-knockdown cells,

we observed an increase in the CXCL13-mediated migration relative to control-knockdown cells, reflecting a decreased adhesion ability of these cells (Figure 5D). No obvious differences in the migration of Mzb1- and control-knockdown MZ B cells were detected on BSA-coated transwell filters. Likewise, integrin-mediated adhesion of Mzb1-knockdown K46 B cells was found to be reduced relative to control and Mzb1*-rescue cells (Figure 5E). The surface expression of the CXCL13 receptor, CXCR5, was not altered on transduced MZ B and K46 B cells (Figures S5A and S5B). Moreover, we detected a reduced surface expression of integrin αLβ2 (LFA-1), which was comparable to that of freshly isolated FoB cells (Figures 6A and 6B). However, the total and surface expression of integrin β1 was similar in Mzb1-siRNA- and control-transduced MZ B cells (Figures 6C and 6D and Figure S6A), raising the question of whether the activation of integrins may be impaired in Mzb1-knockdown cells.

Integrins undergo conformational changes from a bent to an extended structure that reflect differences in the ligand-binding affinities (Luo et al., 2007; Moser et al., 2009). The extended conformation of integrins, which represents the high-affinity receptor, results in a localized “unfolding” of the ectodomain that can be detected by activation state-specific antibodies (Bazzoni et al., 1995). Flow cytometry analysis to detect the extended form of β1 revealed a decrease in the expression of the high-affinity form of VLA-4 in Mzb1-knockdown MZ B cells (Figures 6D). Moreover, lysates from Mzb1-knockdown K46 B cells contained reduced amounts of extended β1 integrin (Figure 6E), consistent with the diminished surface expression on these cells (Figure S6B).

Because ERp57 is involved in the efficient folding of integrins (Jessop et al., 2009), we investigated potential effects of Mzb1 on the isomerization of disulfide bonds in β1 integrin, by using an in vitro folding assay. We added recombinant Mzb1, alone or in combination with ERp57 or BiP as a control, to recombinant VLA-4 in which the disulfide bonds were partially reduced with DTT. Analysis of the conformation of VLA-4 by immunoprecipitation with an activation state-specific anti-β1, followed by immunoblot analysis for β1 integrin detection, indicated that Mzb1 augmented the activity of ERp57 in generating extended β1 integrin (Figures 6F and 6G). However, Mzb1 did not enhance the oxidative folding activity of ERp57 with insulin as a substrate (Figure 6H and Figure S6C). Thus, Mzb1 regulates activity of ERp57 on specific substrates.

Lck-Mzb1 Transgenic T Cells Show Altered Ca^{2+} Mobilization and Cell Adhesion

To examine whether or not Mzb1 can confer alteration of Ca^{2+} mobilization and cell adhesion upon non-B cells in vivo, we generated transgenic mice carrying an *Mzb1* gene under the control of the *Lck*-promoter (Garvin et al., 1990). We confirmed that Mzb1 is not expressed in T cells. With the exception of thymic DN1 stage T cell precursors, none of the other examined T cell populations expressed Mzb1 protein at a detectable level (Figure 7A). Two of three independent transgenic lines expressed Mzb1 at abundant amounts in $CD4^+$ and $CD8^+$ T cells of thymus, lymph node, and spleen (Figure 7B). Analysis of $CD4^+$ and $CD8^+$ T cells by flow cytometry indicated that the ectopic expression of Mzb1 resulted in a modest reduction (~20%) of T cell numbers in lymph nodes and spleen, but did not affect the proportions of the analyzed T cell populations (data not shown). However, stimulation of Mzb1-transgenic $CD4^+$ and $CD8^+$ T cells with anti-CD3ε and anti-CD28 revealed a decreased incorporation of $[H^3]$-thymidine relative to T cells from wild-type littermates (Figure 7C and Figure S7A). Likewise, TCR-induced Ca^{2+} mobilization was reduced in mature T cells of two Mzb1-transgenic lines relative to T cells of a wild-type littermate (Figures 7D and 7E and Figures S7B and S7C). We also observed an impaired nuclear localization of NFAT2 in Mzb1-transgenic $CD4^+$ and $CD8^+$ T cells that have been stimulated with anti-CD3ε and anti-CD28 (Figure 7F and Figures S7D–S7F; Crabtree and Olson, 2002). Finally, we examined LFA-1-mediated adhesion in Mzb1-transgenic $CD4^+$

and $CD8^+$ T cells by static adhesion assays in the presence or absence of CXCL12. In unstimulated wild-type T cells, a moderate adhesion to the LFA-1 ligand ICAM-1 was observed, which could be increased by treatment of cells with CXCL12. However, in Mzb1-expressing T cells, we observed an increase in adhesion to ICAM-1 in the absence or presence of CXCL12 (Figure 7G and Figure S7G). Moreover, we detected a modestly increased surface expression of LFA-1 (Figure 7H and Figure S7H). Taken together, these data suggest that the expression of Mzb1 is sufficient to confer changes in Ca^{2+} mobilization and integrin-mediated cell adhesion.

DISCUSSION

Our analysis of Mzb1 indicates that this cell-type-specific luminal ER protein regulates at least three functions of peripheral B cells. First, Mzb1 controls Ca^{2+} homeostasis and the ER Ca^{2+} store, as evidenced by the enhanced ER Ca^{2+} depletion and extracellular Ca^{2+} influx in thapsigargin-stimulated Mzb1-knockdown K46 B cells. A converse effect on Ca^{2+} fluxes was observed in Mzb1-overexpressing FoB cells and NIH 3T3 cells, as well as in Mzb1-transgenic T cells. The altered Ca^{2+} homeostasis in cells in which Mzb1 has been down- or upregulated could be accounted for by the interaction of Mzb1 with the SERCA pump and one of its regulators, the oxidoreductase ERp57 (Li and Camacho, 2004). The regulation of the ER Ca^{2+} store by Mzb1 is probably related to the effects of altered Mzb1 expression on the nuclear localization of NFAT2, which is modulated by the Ca^{2+} and calmodulin-dependent serine-threonine phosphatase calcineurin (Crabtree and Olson, 2002). Knockdown of Mzb1 in MZ B and B1 cells enhanced nuclear localization of NFAT2, whereas overexpression of Mzb1 in FoB cells or transgenic T cells impaired nuclear localization of NFAT2. Changes in Ca^{2+} signaling and NFAT activity have been attributed to the proliferative response of B cells. In particular, NFAT2-deficient mice show a compromised B cell proliferation in vitro (Ranger et al., 1998). Likewise, the mutation of the regulatory subunit of calcineurin in B cells results in a cell-autonomous defect in cell proliferation (Winslow et al., 2006). In primary MZ B cells and in K46 B cells, the knockdown of Mzb1 increased cell proliferation, whereas the overexpression of Mzb1 in FoB cells decreased cell proliferation and BCR-mediated Ca^{2+} mobilization, suggesting that Mzb1 sets a threshold for Ca^{2+} signaling. Peripheral B cell subsets differ in their cellular responses to BCR signaling (Casola et al., 2004). The Mzb1-mediated changes of the homeostatic ER Ca^{2+} concentration are consistent with the anergic state of B1 cells and the weak signal dependence of MZ B cells (Dal Porto et al., 2004; Pillai and Cariappa, 2009). Therefore, Mzb1 may indirectly contribute to cell-type-specific differences in BCR signal transduction.

Second, Mzb1 affects the secretion of antibodies in LPS-stimulated B lymphocytes, but not the transcriptional response to LPS. Moreover, LPS-stimulated FoB cells upregulate Mzb1 expression with kinetics that resemble that of antibody secretion (data not shown), and the forced expression of Mzb1 in FoB cells accelerates and augments immunoglobulin secretion. The recent finding that pERp1(Mzb1) knockdown in plasmacytoma cells has at most a 2-fold effect on antibody secretion (van Anken et al., 2009) suggests that the effect of Mzb1 on immunoglobulin secretion may be restricted to stimulation via TLRs and/or limited to primary cells. The observed changes in antibody secretion in Mzb1-knockdown cells may be accounted for by the association of Mzb1 with ERp57 and Grp94. Moreover, in Mzb1-knockdown MZ B cells, TLR4 surface expression is downregulated, raising the possibility that the impaired antibody secretion could reflect a combined defect in TLR surface expression and immunoglobulin folding.

Third, Mzb1 has a role in the integrin-mediated adhesion of MZ B cells and T cells. We find that downregulation of Mzb1 in MZ B cells impairs the chemokine-induced adhesion to the

integrin ligands VCAM-1 or ICAM-1. Conversely, ectopic expression of Mzb1 in T cells is sufficient for increasing integrin-mediated cell adhesion. Interestingly, a major function of Mzb1 in regulating the activity of integrins is the transition of the bent conformation to the extended conformation, which has been shown to represent the activation-competent state (Hynes, 2002; Luo et al., 2007). In addition, we observe changes in the surface expression of the integrins αL and β2. The marked effect of Mzb1 downregulation on the activation of integrins appears to be related to the association of Mzb1 with ERp57. Notably, we find that Mzb1 augments the oxidoreductase activity of ERp57 on integrin β1 in vitro, but does not enhance its activity on insulin, suggesting that Mzb1 confers substrate specificity upon ERp57.

How can Mzb1 affect multiple cellular processes? Mzb1 has no structural hallmarks besides a CXXC thioredoxin motif. However, we could not detect any marked oxidoreductase activity of Mzb1 by itself in vitro, and mutation of one cysteine of the CXXC motif had no pronounced effect on the function of Mzb1 in regulating Ca^{2+} signaling. The interaction partner of Mzb1, ERp57, exists in a complex with calreticulin and calnexin whereby these lectin chaperones mediate a broad substrate recognition (Appenzeller-Herzog and Ellgaard, 2008; Jessop et al., 2009). However, the mass spectrometric analysis of Mzb1-associated proteins suggested that Mzb1 interacts with the Grp94-BiP multichaperone complex and ERp57 in the absence of the calreticulin and calnexin chaperones. Moreover, an exchange of the ERp57-associated chaperones by Mzb1 is supported by the coimmunoprecipitation of calnexin and calreticulin with ERp57 antibody in Mzb1-knockdown cells, whereas Grp94 is preferentially coimmunoprecipitated in control and Mzb1*-rescue cells.

Various biological processes have been shown to depend on both ERp57 and Grp94. MHC class I assembly requires both proteins, and the enzymatic activity of ERp57 undergoes a transient change upon covalent linkage with tapasin (Wearsch and Cresswell, 2008). In this context, ERp57 acts in concert with tapasin, independently of its partners calreticulin and calnexin. Moreover, both ERp57 and Grp94 regulate ER Ca^{2+} homeostasis. Although multiple ER proteins have a high capacity for Ca^{2+} binding, Grp94 appears to have a unique effect on the ER Ca^{2+} store. In particular, Grp94-deficient but not calreticulin-deficient cells are hypersensitive to perturbations in Ca^{2+} stores (Biswas et al., 2007). The specific effect of Grp94 on Ca^{2+} homeostasis has been interpreted to suggest that Grp94 physically or functionally interacts with Ca^{2+} pumps, Ca^{2+} leakage channels, or a regulatory protein. Mzb1 may regulate the recruitment of Grp94 and ERp57 to SERCA2b, which was also identified in our proteomic analysis. The association of Mzb1 with ERp57 and SERCA2b may also explain why Mzb1 has negative roles in Ca^{2+} fluxes and cell proliferation, whereas it has a positive role in integrin activation and antibody secretion. ERp57 has been shown to inhibit the activity of SERCA2b by interacting with its intraluminal loop L4 (Li and Camacho, 2004). Moreover, overexpression of ERp57 reduces the frequency of SERCA2b-dependent Ca^{2+} oscillations in *Xenopus* oocytes and overexpression of SERCA2b variants with mutated cysteines located in loop L4 increases the frequency of Ca^{2+} oscillation. In this context, ERp57 does not affect the activity of SERCA2b mutants lacking the calreticulin-binding site (Li and Camacho, 2004).

If the function of Mzb1 involves the association with ERp57 and Grp94 in vivo, one might expect some overlap of phenotypes observed in B cells with altered Mzb1, ERp57, or Grp94 expression. TLR-stimulated, Grp94-deficient B cells display an attenuated antibody production, whereby the defect has been attributed to a diminished surface expression of TLR (Liu and Li, 2008). Moreover, Grp94-deficient B cells show a selective loss of the surface expression of α4 and αL integrins (Liu and Li, 2008; Randow and Seed, 2001), consistent with the effects of Mzb1 downregulation on integrin expression and function. ERp57-deficient B cells show a defect in antigen presentation but have no major phenotype

in cell proliferation or antibody secretion (Garbi et al., 2006). However, this study did not examine a potential role of ERp57 in “innate-like” B cells and integrin function. The association of Mzb1 with components of a multichaperone complex is also intriguing in light of the ability of chaperone proteins to promote rapid changes in phenotypic traits and to allow selection to act on multiple processes at one time (Rutherford, 2003). Therefore, Mzb1 may have been involved in diversifying the immune functions of peripheral B cell subsets.

EXPERIMENTAL PROCEDURES

Mzb1 Knockdown and Retroviral Transduction

siRNA duplexes were designed using the Invitrogen BLOCK-iT program. Mzb1-specific duplex 5′-GCGAAAGCAGAGGCUAAAU-3′ and a scrambled control siRNA duplex 5′-GUACCUUGACAGUACCGAU-3′ were cloned into the pSuper RNAi system (OligoEngine). Stable clones for both siRNA duplexes were generated, and the siRNA clone revealing the most efficient Mzb1-knockdown clone (clone #10) was stably transfected with either a siRNA-resistant *Mzb1* cDNA (Mzb1*) or a mutated, siRNA-resistant *Mzb1* cDNA, carrying a cysteine to alanine mutation at position 52 (Mzb1$*^{CXXA}$). For knockdown of Mzb1 in FACS-sorted B220^{+}CD21^{hi}CD23^{-} MZ B, B220^{+}CD21^{int}CD23^{hi} FoB or peritoneal CD19^{+}CD5^{+}CD23^{-} B1 B cells (FACS antibodies acquired from BD Biosciences), the Mzb1-specific siRNA duplex and the scrambled control siRNA duplex were integrated into a modified version of the GFP bicistronic pEGZ-MCS retroviral vector and the GP+E86 packaging cell line was transfected with the retroviral reporter plasmids (Markowitz et al., 1988). For infection of MZ B, FoB, or B1 B cells, mitomycin C-inactivated GP+E86 packaging cells were plated to confluency on gelatinized cell culture plates and the lymphocytes were cocultured with the inactivated GP+E86 feeders in RPMI 1640 media supplemented with polybrene (2 μg/ml) at 5% CO_2 and 37°C for 48 hr. After infection, GFP-positive lymphocytes were enriched. For overexpression of Mzb1 in FoB or MZ B cells, *Mzb1* cDNA was cloned into the GFP bicistronic pEGZ/MCS retroviral vector and the cells were transduced as described above.

Transwell Assay

Chemotaxis assays of siControl- and siMzb1-MZ B cells or siControl-, siMzb1-, and siMzb1+Mzb1*-transfected K46 cells to CXCL13 (R&D Systems) were performed as described (Lu and Cyster, 2002). In brief, transduced MZ B cells or K46 B cells were enriched for GFP-positive cells and resuspended in RPMI 1640 media for primary lymphocytes, and 1×10^5 cells (per well) were placed in 5 μm (MZ) or 8 μm (K46) transwell chemotaxis chambers (Corning Costar). The chambers were coated for 1 hr with BSA (0.25% in PBS), ICAM-1 (3 μg/ml in PBS; R&D Systems), or VCAM-1 (3 μg/ml in PBS; R&D Systems), washed two times with 0.1% BSA in RPMI 1640, and blocked with 0.5% BSA in RPMI 1640. Cells were incubated in the coated chambers for 3 hr at 37°C and 5% CO_2. Cells that migrated to the lower chamber, containing 0, 0.1 or 0.5 μg/ml CXCL13, were counted by collecting events for a fixed time (60 s) on a FACS Calibur flow cytometer.

Supplementary Material

Refer to Web version on PubMed Central for supplementary material.

Acknowledgments

We thank I. Falk for expert technical help, A. Travis for the initial screening of the cDNA library, B. Schreiber and M. Pink for their help in generating the siRNA knockdown cells, K. Rattay for help in establishing the isomerization assay and E. Kremmer (GSF, Munich) for producing Mzb1 monoclonal antibodies. We thank M. Digman and E. Gratton for assistance with the fluorescence lifetime imaging measurements. We are grateful to R.

Faessler, S. Rospert, A. Spang, H.P. Hauri, W. Schamel and M. Reth for discussions and advice. We thank R. Faessler, U. Hartl and E. Mandel for comments on the manuscript. S.K. was supported by a Danish Graduate Student Fellowship. This work was supported by funds of the Max-Planck-Research-Society.

REFERENCES

Allman D, Pillai S. Peripheral B cell subsets. Curr. Opin. Immunol. 2008; 20:149–157. [PubMed: 18434123]

Ansel KM, Harris RB, Cyster JG. CXCL13 is required for B1 cell homing, natural antibody production, and body cavity immunity. Immunity. 2002; 16:67–76. [PubMed: 11825566]

Appenzeller-Herzog C, Ellgaard L. The human PDI family: Versatility packed into a single fold. Biochim. Biophys. Acta. 2008; 1783:535–548. [PubMed: 18093543]

Bazzoni G, Shih DT, Buck CA, Hemler ME. Monoclonal antibody 9EG7 defines a novel beta 1 integrin epitope induced by soluble ligand and manganese, but inhibited by calcium. J. Biol. Chem. 1995; 270:25570–25577. [PubMed: 7592728]

Biswas C, Ostrovsky O, Makarewich CA, Wanderling S, Gidalevitz T, Argon Y. The peptide-binding activity of GRP94 is regulated by calcium. Biochem. J. 2007; 405:233–241. [PubMed: 17411420]

Cahalan MD. STIMulating store-operated Ca(2+) entry. Nat. Cell Biol. 2009; 11:669–677. [PubMed: 19488056]

Casola S, Otipoby KL, Alimzhanov M, Humme S, Uyttersprot N, Kutok JL, Carroll MC, Rajewsky K. B cell receptor signal strength determines B cell fate. Nat. Immunol. 2004; 5:317–327. [PubMed: 14758357]

Chumley MJ, Dal Porto JM, Cambier JC. The unique antigen receptor signaling phenotype of B-1 cells is influenced by locale but induced by antigen. J. Immunol. 2002; 169:1735–1743. [PubMed: 12165494]

Crabtree GR, Olson EN. NFAT signaling: Choreographing the social lives of cells. Cell Suppl. 2002; 109:S67–S79.

Dal Porto JM, Burke K, Cambier JC. Regulation of BCR signal transduction in B-1 cells requires the expression of the Src family kinase Lck. Immunity. 2004; 21:443–453. [PubMed: 15357954]

Ellgaard L, Ruddock LW. The human protein disulphide isomerase family: Substrate interactions and functional properties. EMBO Rep. 2005; 6:28–32. [PubMed: 15643448]

Garbi N, Tanaka S, Momburg F, Hammerling GJ. Impaired assembly of the major histocompatibility complex class I peptide-loading complex in mice deficient in the oxidoreductase ERp57. Nat. Immunol. 2006; 7:93–102. [PubMed: 16311600]

Garvin AM, Abraham KM, Forbush KA, Farr AG, Davison BL, Perlmutter RM. Disruption of thymocyte development and lymphoma-genesis induced by SV40 T-antigen. Int. Immunol. 1990; 2:173–180. [PubMed: 1965144]

Genestier L, Taillardet M, Mondiere P, Gheit H, Bella C, Defrance T. TLR agonists selectively promote terminal plasma cell differentiation of B cell subsets specialized in thymus-independent responses. J. Immunol. 2007; 178:7779–7786. [PubMed: 17548615]

Ghadially H, Ross XL, Kerst C, Dong J, Reske-Kunz AB, Ross R. Differential regulation of CCL22 gene expression in murine dendritic cells and B cells. J. Immunol. 2005; 174:5620–5629. [PubMed: 15843561]

Hardy RR, Kincade PW, Dorshkind K. The protean nature of cells in the B lymphocyte lineage. Immunity. 2007; 26:703–714. [PubMed: 17582343]

Hynes RO. Integrins: Bidirectional, allosteric signaling machines. Cell. 2002; 110:673–687. [PubMed: 12297042]

Jessop CE, Tavender TJ, Watkins RH, Chambers JE, Bulleid NJ. Substrate specificity of the oxidoreductase ERp57 is determined primarily by its interaction with calnexin and calreticulin. J. Biol. Chem. 2009; 284:2194–2202. [PubMed: 19054761]

Kinashi T. Intracellular signalling controlling integrin activation in lymphocytes. Nat. Rev. Immunol. 2005; 5:546–559. [PubMed: 15965491]

Kolb JP, Renard D, Dugas B, Genot E, Petit-Koskas E, Sarfati M, Delespesse G, Poggioli J. Monoclonal anti-CD23 antibodies induce a rise in [Ca2+]i and polyphosphoinositide hydrolysis in

human activated B cells. Involvement of a Gp protein. J. Immunol. 1990; 145:429–437. [PubMed: 2164062]

Li Y, Camacho P. Ca2+-dependent redox modulation of SERCA 2b by ERp57. J. Cell Biol. 2004; 164:35–46. [PubMed: 14699087]

Liu B, Li Z. Endoplasmic reticulum HSP90b1 (gp96, grp94) optimizes B-cell function via chaperoning integrin and TLR but not immunoglobulin. Blood. 2008; 112:1223–1230. [PubMed: 18509083]

Lu TT, Cyster JG. Integrin-mediated long-term B cell retention in the splenic marginal zone. Science. 2002; 297:409–412. [PubMed: 12130787]

Luik RM, Wang B, Prakriya M, Wu MM, Lewis RS. Oligomerization of STIM1 couples ER calcium depletion to CRAC channel activation. Nature. 2008; 454:538–542. [PubMed: 18596693]

Luo BH, Carman CV, Springer TA. Structural basis of integrin regulation and signaling. Annu. Rev. Immunol. 2007; 25:619–647. [PubMed: 17201681]

Markowitz D, Goff S, Bank A. A safe packaging line for gene transfer: Separating viral genes on two different plasmids. J. Virol. 1988; 62:1120–1124. [PubMed: 2831375]

Martin F, Kearney JF. B-cell subsets and the mature preimmune repertoire. Marginal zone and B1 B cells as part of a “natural immune memory”. Immunol. Rev. 2000; 175:70–79. [PubMed: 10933592]

Melnick J, Dul JL, Argon Y. Sequential interaction of the chaperones BiP and GRP94 with immunoglobulin chains in the endoplasmic reticulum. Nature. 1994; 370:373–375. [PubMed: 7913987]

Moser M, Legate KR, Zent R, Fassler R. The tail of integrins, talin, and kindlins. Science. 2009; 324:895–899. [PubMed: 19443776]

Muller G, Lipp M. Signal transduction by the chemokine receptor CXCR5: Structural requirements for G protein activation analyzed by chimeric CXCR1/CXCR5 molecules. Biol. Chem. 2001; 382:1387–1397. [PubMed: 11688722]

Ni M, Lee AS. ER chaperones in mammalian development and human diseases. FEBS Lett. 2007; 581:3641–3651. [PubMed: 17481612]

Pillai S, Cariappa A. The follicular versus marginal zone B lymphocyte cell fate decision. Nat. Rev. Immunol. 2009; 9:767–777. [PubMed: 19855403]

Randow F, Seed B. Endoplasmic reticulum chaperone gp96 is required for innate immunity but not cell viability. Nat. Cell Biol. 2001; 3:891–896. [PubMed: 11584270]

Ranger AM, Hodge MR, Gravallese EM, Oukka M, Davidson L, Alt FW, de la Brousse FC, Hoey T, Grusby M, Glimcher LH. Delayed lymphoid repopulation with defects in IL-4-driven responses produced by inactivation of NF-ATc. Immunity. 1998; 8:125–134. [PubMed: 9462518]

Richards S, Watanabe C, Santos L, Craxton A, Clark EA. Regulation of B-cell entry into the cell cycle. Immunol. Rev. 2008; 224:183–200. [PubMed: 18759927]

Rubtsov AV, Swanson CL, Troy S, Strauch P, Pelanda R, Torres RM. TLR agonists promote marginal zone B cell activation and facilitate T-dependent IgM responses. J. Immunol. 2008; 180:3882–3888. [PubMed: 18322196]

Rutherford SL. Between genotype and phenotype: Protein chaperones and evolvability. Nat. Rev. Genet. 2003; 4:263–274. [PubMed: 12671657]

Sebzda E, Bracke M, Tugal T, Hogg N, Cantrell DA. Rap1A positively regulates T cells via integrin activation rather than inhibiting lymphocyte signaling. Nat. Immunol. 2002; 3:251–258. [PubMed: 11836528]

Shimizu Y, Meunier L, Hendershot LM. pERp1 is significantly up-regulated during plasma cell differentiation and contributes to the oxidative folding of immunoglobulin. Proc. Natl. Acad. Sci. USA. 2009; 106:17013–17018. [PubMed: 19805157]

Todd DJ, Lee AH, Glimcher LH. The endoplasmic reticulum stress response in immunity and autoimmunity. Nat. Rev. Immunol. 2008; 8:663–674. [PubMed: 18670423]

Travis A, Amsterdam A, Belanger C, Grosschedl R. LEF-1, a gene encoding a lymphoid-specific protein with an HMG domain, regulates T-cell receptor alpha enhancer function. Genes Dev. 1991; 5:880–894. [PubMed: 1827423]

Tu BP, Weissman JS. Oxidative protein folding in eukaryotes: Mechanisms and consequences. J. Cell Biol. 2004; 164:341–346. [PubMed: 14757749]

Tumang JR, Frances R, Yeo SG, Rothstein TL. Spontaneously Ig-secreting B-1 cells violate the accepted paradigm for expression of differentiation-associated transcription factors. J. Immunol. 2005; 174:3173–3177. [PubMed: 15749846]

van Anken E, Pena F, Hafkemeijer N, Christis C, Romijn EP, Grauschopf U, Oorschot VM, Pertel T, Engels S, Ora A, et al. Efficient IgM assembly and secretion require the plasma cell induced endoplasmic reticulum protein pERp1. Proc. Natl. Acad. Sci. USA. 2009; 106:17019–17024. [PubMed: 19805154]

Vig M, Kinet JP. Calcium signaling in immune cells. Nat. Immunol. 2009; 10:21–27. [PubMed: 19088738]

Wearsch PA, Cresswell P. The quality control of MHC class I peptide loading. Curr. Opin. Cell Biol. 2008; 20:624–631. [PubMed: 18926908]

Winslow MM, Gallo EM, Neilson JR, Crabtree GR. The calcineurin phosphatase complex modulates immunogenic B cell responses. Immunity. 2006; 24:141–152. [PubMed: 16473827]

Won WJ, Kearney JF. CD9 is a unique marker for marginal zone B cells, B1 cells, and plasma cells in mice. J. Immunol. 2002; 168:5605–5611. [PubMed: 12023357]

Wong SC, Chew WK, Tan JE, Melendez AJ, Francis F, Lam KP. Peritoneal CD5+ B-1 cells have signaling properties similar to tolerant B cells. J. Biol. Chem. 2002; 277:30707–30715. [PubMed: 12070149]

Yang Y, Li Z. Roles of heat shock protein gp96 in the ER quality control: Redundant or unique function? Mol. Cells. 2005; 20:173–182. [PubMed: 16267390]

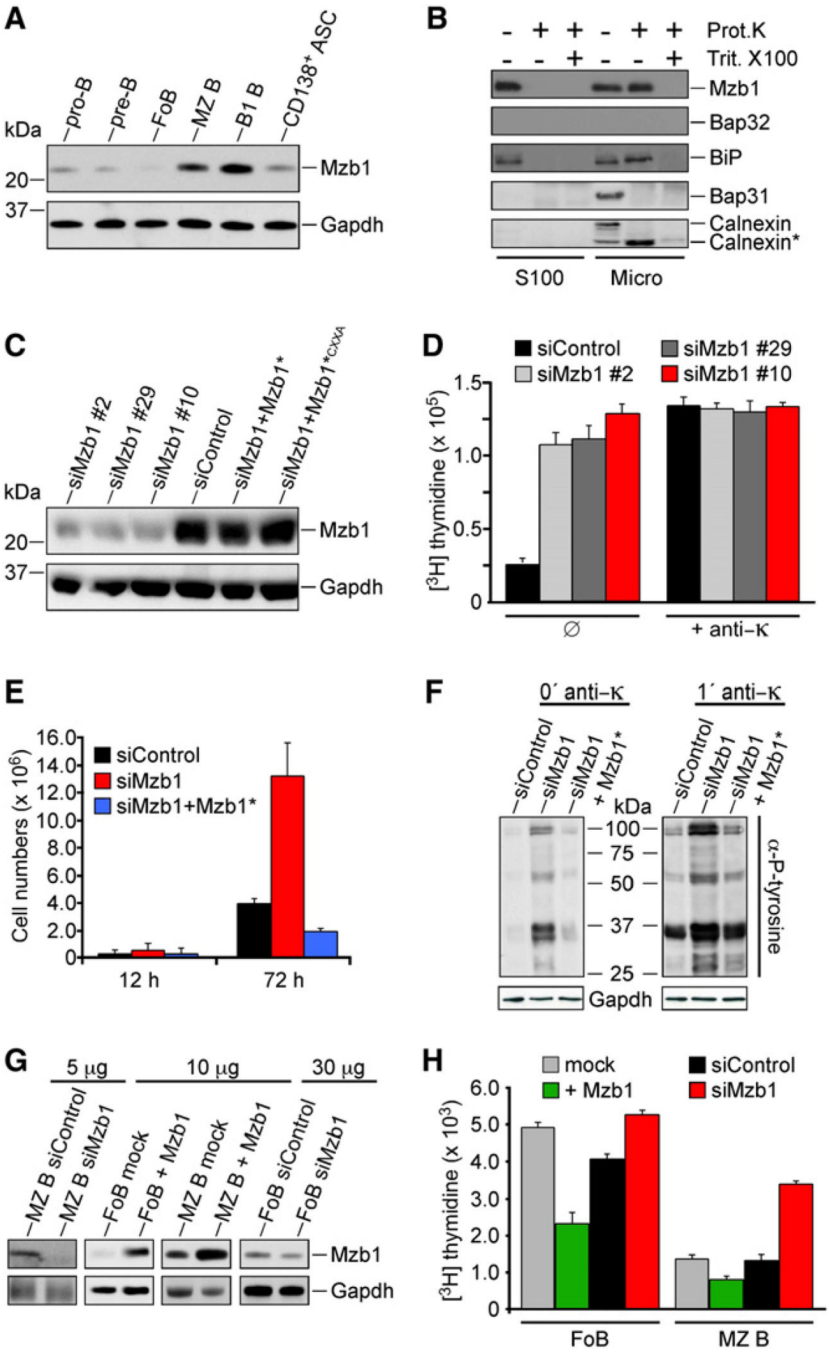

Figure 1. Mzb1, a MZ B and B1 Cell-Specific ER Protein, Regulates Cell Proliferation

(A) Immunoblot analysis with a monoclonal Mzb1-specific antibody of total protein extracts of flow cytometer-sorted primary B cell populations (ASC, antibody-secreting cells).

(B) Immunoblot analysis of K46 B cell microsomal fractions (Micro) and corresponding supernatants (S100).

(C) Immunoblot analysis of lysates from K46 cells stably transfected with plasmids expressing siControl, siMzb1 (clones #2, #29, and #10), siMzb1+ cleavage-resistant Mzb1*, or siMzb1+Mzb1*^{CXXA}.

(D and E) Cell proliferation analysis of siControl−, siMzb1− and siMzb1+Mzb1*-transfected K46 cells.

(D) [^{3}H] thymidine incorporation was determined in cells without (ø) or with anti-κ stimulation (5 μg/ml) for 16 hr. Data are expressed as the mean [^{3}H] thymidine incorporation of triplicate cultures and are representative of three independent experiments. Error bars indicate SD of the mean.

(E) Cell numbers after 12 hr and 72 hr. The data represent mean values of triplicate cultures and are representative of three independent experiments.

(F) Analysis of tyrosine phosphorylation in serum-deprived and anti-κ-stimulated Mzb1-knockdown K46 B cells. Phosphotyrosine-modified proteins were detected by immunoblot analysis; n = 3.

(G and H) Analysis of cell proliferation of FoB or MZ B cells transduced with GFP-bicistronic retroviruses expressing Mzb1, siMzb1, or siControl.

(G) Immunoblot analysis for detecting Mzb1 or GAPDH in total cell lysates (5–30 μg/lane) of sorted GFP-positive FoB or MZ B cells that were transduced with Mzb1- or siMzb1-expressing retroviruses.

(H) Analysis of [^{3}H] thymidine incorporation in retrovirally transduced and GFP-sorted FoB or MZ B cells (mean of triplicate cultures). The data are representative of three independent experiments and error bars indicate SD of the mean.

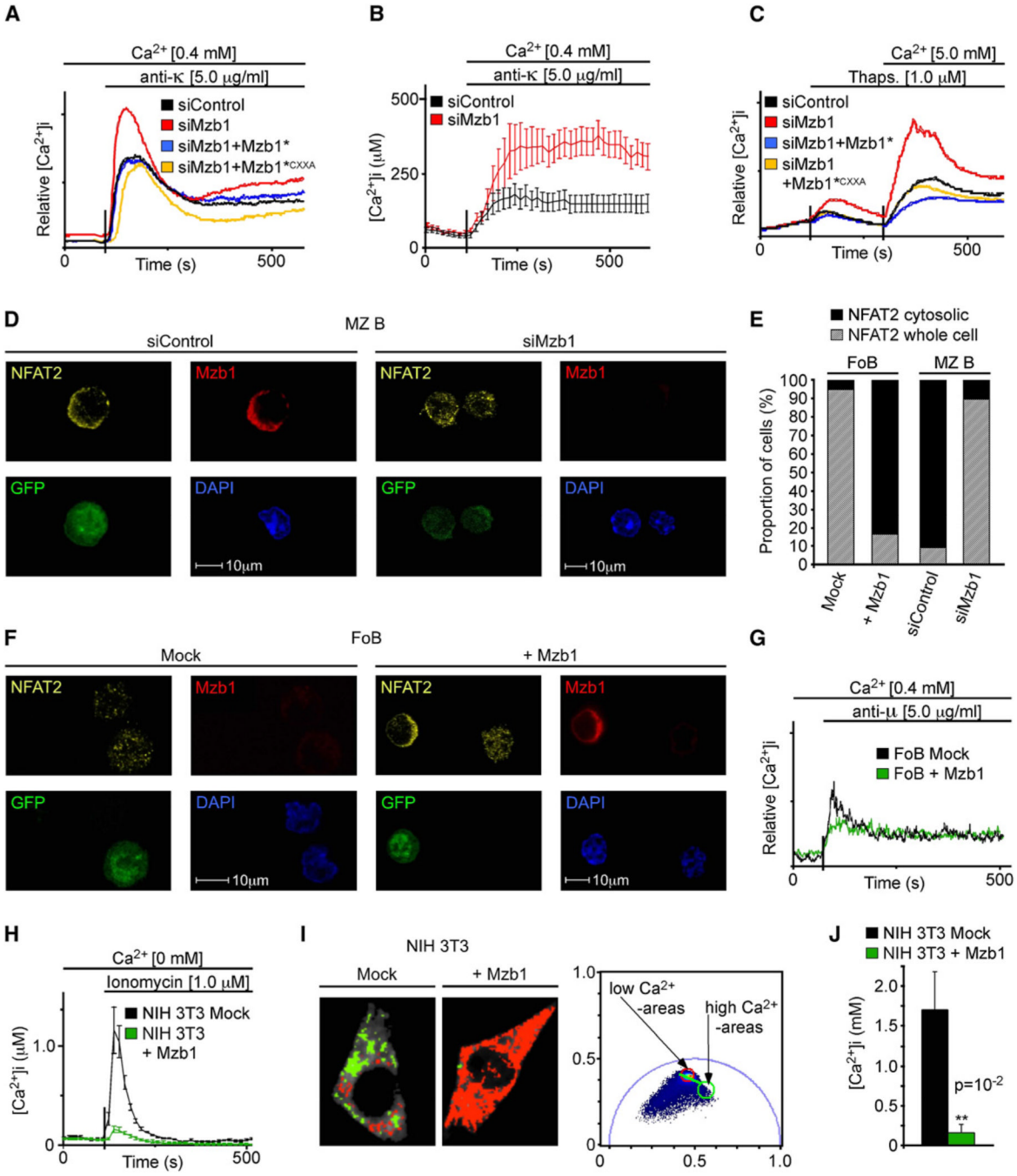

Figure 2. Mzb1 Expression Decreases the Luminal ER Ca^{2+} Store Content

(A–C) Analysis of experimentally-induced Ca^{2+} fluxes in K46 B cells stably transfected with siControl, siMzb1, siMzb1+Mzb1*, and siMzb1+Mzb1*^{CXXA} plasmids. Indo-1AM-loaded cells were treated (A) with anti-κ or (C) thapsigargin and increases in free intracellular Ca^{2+} were measured in real time. Data are representative of five independent experiments.

(B) Average $[Ca^{2+}]_i$ responses in individual BCR-stimulated siControl-K46 (n = 17) or siMzb1-K46 (n = 7) cells. Error bars indicate SD of the mean.

(D) Indirect immunofluorescence analysis of flow cytometer-sorted GFP-positive mock- or Mzb1-transduced MZ B cells with anti-Mzb1 and anti-NFAT2.

(E) Quantification of the proportion of mock- or Mzb1-transduced GFP-positive FoB cells ($n \geq 120$ per genotype) and of siControl- or siMzb1-transduced GFP-positive MZB cells ($n \geq 90$ per genotype) showing NFAT2 protein distributed over the whole cell (hatched bar) or concentrated in the cytosolic compartment (solid bar). GFP served as a marker for transduction and DAPI defined the nuclear area.
(F) Indirect immunofluorescence using siControl- or siMzb1-transduced, GFP-positive FoB cells, as described previously.
(G) Analysis of anti-μ induced Ca^{2+} fluxes in mock- or Mzb1-transduced FoB cells as described above. Data are representative of five independent experiments.
(H) Average $[Ca^{2+}]_i$ responses in individual ionomycin-treated NIH 3T3 cells stably transfected with a mock- or Mzb1-expression plasmid.
(I and J) Fluorescence lifetime imaging microscopy (FLIM) to directly determine the ER Ca^{2+} store content in stably mock- or Mzb1-transfected NIH 3T3 cells transiently transfected with the ER-localized cameleon (YC4.2er). In (I), the phasor plot (right panel) of the FLIM images shown in the two left panels represents the two basic forms of the YC4.2er: one in the absence of Ca^{2+} having a long lifetime (red circle; red pixels in FLIM image) and one in the calcium binding state that shortens its lifetime (green circle; green pixels in FLIM image).
(J) Representation of the data obtained by the phasor approach as Ca^{2+} concentrations with the “Globals for Images” software with $n_{(NIH\ 3T3\ mock)} = 4$ and $n_{(NIH\ 3T3\ +\ Mzb1)} = 5$ ($p = 10^{-2}$). Error bars indicate SD of the mean and the significance was determined by a two-tailed t test.

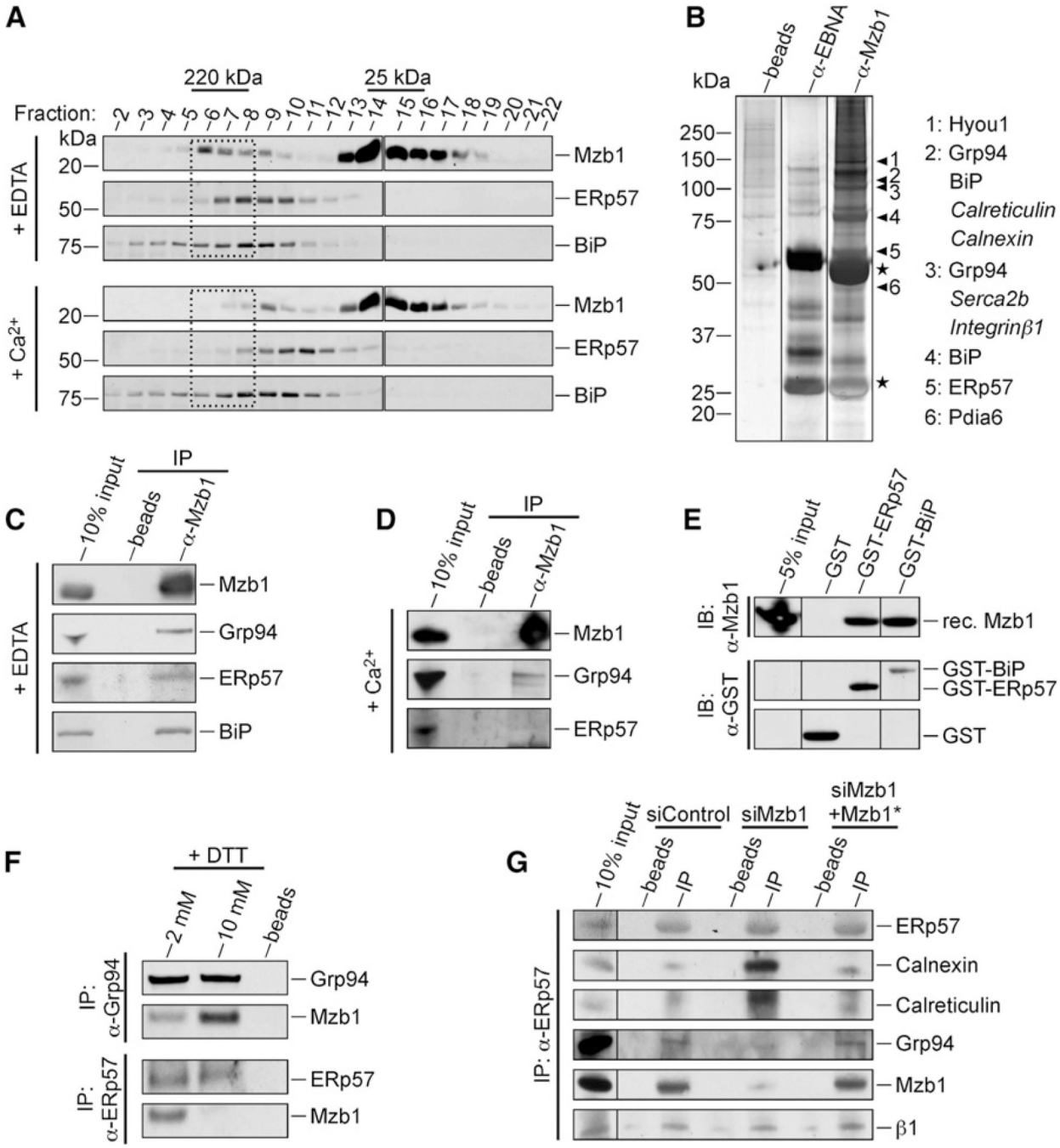

Figure 3. Proteomic Analysis of Mzb1-Associated Proteins

(A) Gel filtration analysis of NP40-solubilized microsomes of K46 B cells in the absence (10 mM EDTA) or presence (2.5 mM Ca^{2+}) of calcium. Mzb1 and Mzb1-containing complexes in individual fractions were visualized by immunoblot analysis for detecting Mzb1, ERp57, and BiP.

(B) In vivo cross-linking and affinity purification of Mzb1-associated proteins from thapsigargin-(1 μM) and EGTA- (3 mM) treated K46 B cells. After whole-cell extract preparation and immunoprecipitation with anti-Mzb1 or anti-EBNA coupled to sepharose beads, crosslinks were reversed and the proteins separated on a 4%–12% SDS-PAGE gel and visualized by silver stain. Lanes are from the same gel. Specific bands were cut out and

analyzed by mass-spectrometry with the protein identities shown. High and low protein abundance is indicated by plain or italic letters, respectively.
(C and D) Coimmunoprecipitation analysis of K46 protein extract to detect association of Mzb1 with Grp94, ERp57 and BiP in the (C) absence (10 mM EDTA) or (D) presence (2.5 mM Ca^{2+}) of calcium, with anti-Mzb1 antibody for precipitation.
(E) GST-pulldown assay with recombinant Mzb1 protein and glutathione beads coupled to GST, GST-ERp57, or GST-BiP, followed by an immunoblot analysis.
(F) Coimmunoprecipitation analysis of K46 protein extract for analysis of the association of Mzb1 with Grp94 and ERp57 in the presence of DTT.
(G) Coimmunoprecipitation analysis of protein extracts from K46 cells expressing siControl, siMzb1, and siMzb1+Mzb1* plasmids with ERp57 antibody for precipitation. Data are representative of three independent experiments.

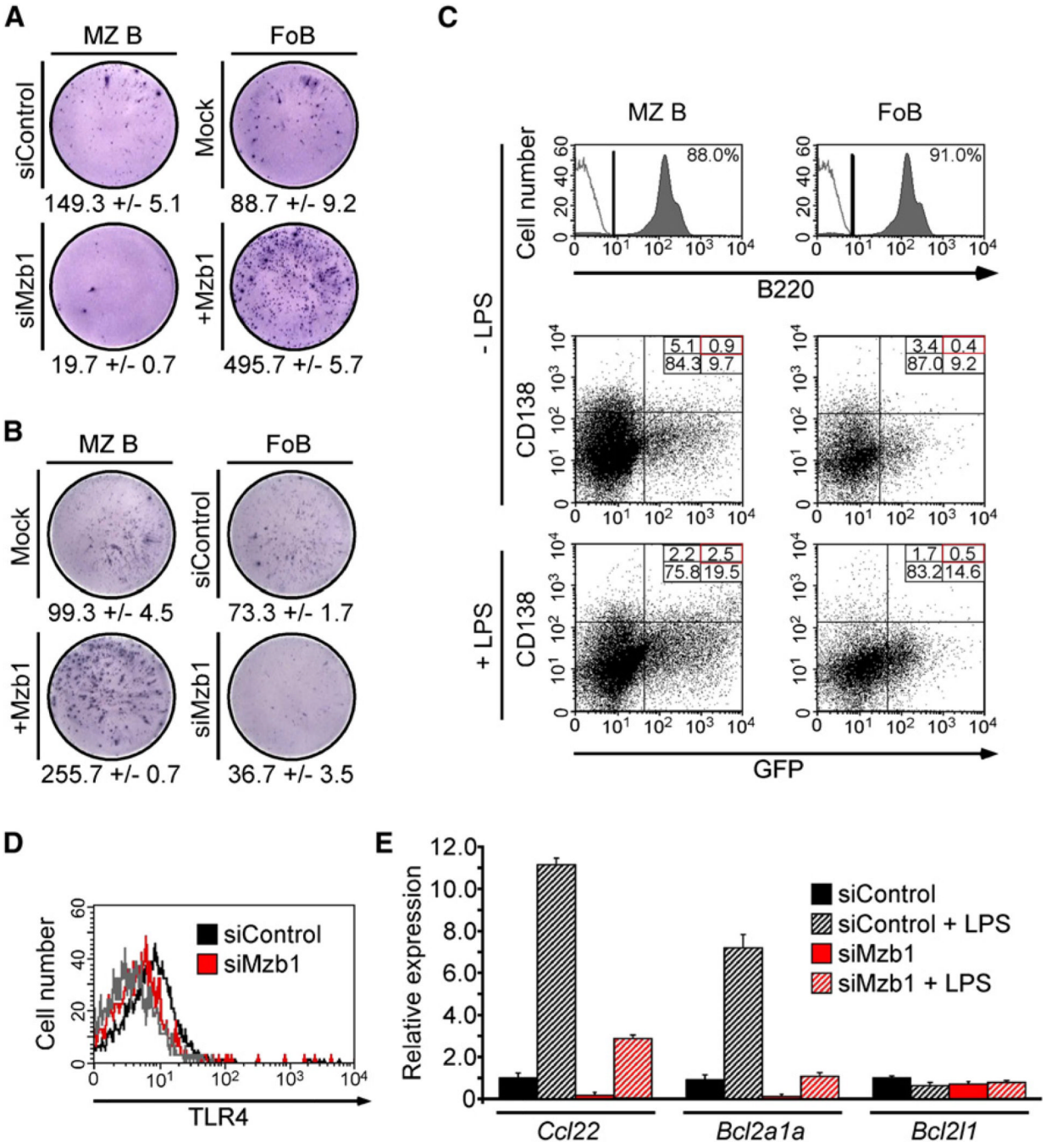

Figure 4. Mzb1 Influences Antibody Secretion

(A and B) ELISpot-analysis to detect IgM antibody-secreting cells in MZ B and FoB cells transduced with a control- or Mzb1-siRNA-expressing retrovirus or with a mock- or Mzb1-expressing retrovirus. Retroviral transductions were performed for 48 hr, whereby LPS (1 μg/ml) was added after 36 hr and GFP-positive cells were sorted and stimulated with LPS (1 μg/ml) for an additional 4 hr. Data represent the mean and SD of triplicate samples and data are representative of three independent experiments.

(C) Flow cytometric analysis of GFP expression and surface CD138 levels on MZ B cells transduced with a Mzb1-siRNA-expressing retrovirus (left panels) and on FoB cells transduced with a Mzb1-expressing retrovirus (right panels). Cells were either infected in

the absence of LPS (upper four panels) or infected for 24 hr in the absence of LPS and then stimulated with 1 μg/ml of LPS for 24 hr (lower two panels). Flow cytometry dot plots reflect living B220-positive cells with the B220-gate shown in the two histograms. The solid gray line represents the isotype control (two upper panels) and data are representative of three independent experiments.

(D) Flow cytometric analysis of surface TLR4 on siControl- or siMzb1-expressing MZ B cells. The solid gray line represents the isotype control and FACS profiles reflect living, GFP-positive cells.

(E) Quantitative RT-PCR analysis of *Ccl22*, *Bcl2a1a*, and *Bcl2l1* transcripts in siControl- or siMzb1-MZ B cells. GFP-positive cells were sorted and left untreated or stimulated with LPS (1 μg/ml) for 24 hr. Relative expression is normalized to *actin* (n = 3).

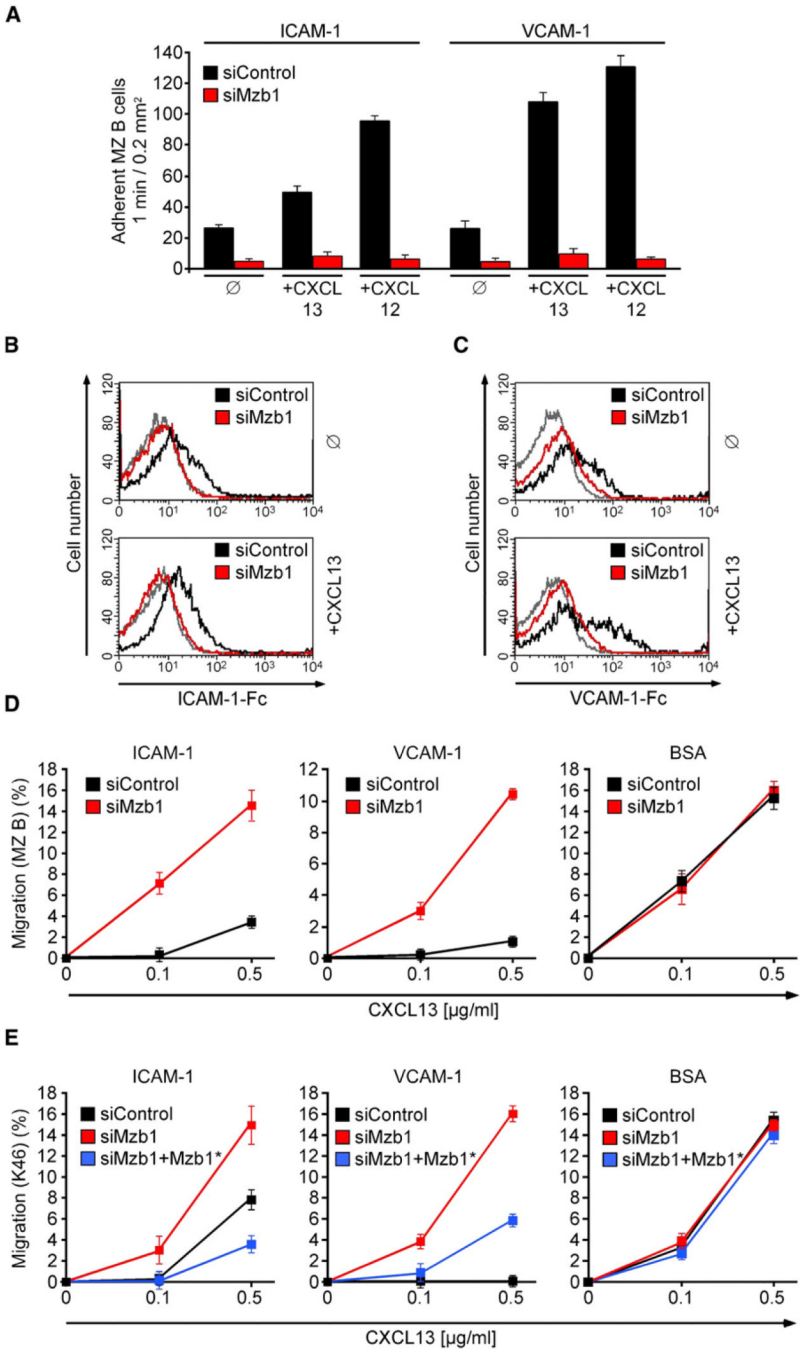

Figure 5. Mzb1 Regulates Integrin-Mediated Cell Adhesion

(A) Static adhesion to ICAM-1 or VCAM-1. SiControl- or siMzb1-MZ B cells were treated with buffer (ø) or stimulated with CXCL13 or CXCL12. Assays were performed in triplicate, and data are representative of three independent experiments. Error bars indicate SD of the mean.

(B and C) LFA-1 and VLA-4 affinity assays with siControl- or siMzb1-MZ B cells. The histograms show the relative ability of untreated (ø) or CXCL13-stimulated, GFP-positive MZ B cells to bind soluble (B) ICAM-1-Fc or (C) VCAM-1-Fc.

(D) Chemotaxis assay of siControl- or siMzb1-MZ B cells. GFP-positive cells were placed in transwell chambers coated with ICAM-1, VCAM-1, or BSA and allowed to migrate

toward CXCL13. Assays were performed in duplicate, and data are representative of at least three independent experiments. Error bars indicate SD of the mean.
(E) Chemotaxis assay of siControl-, siMzb1-, and siMzb1+Mzb1*-K46 cells as described in (D).

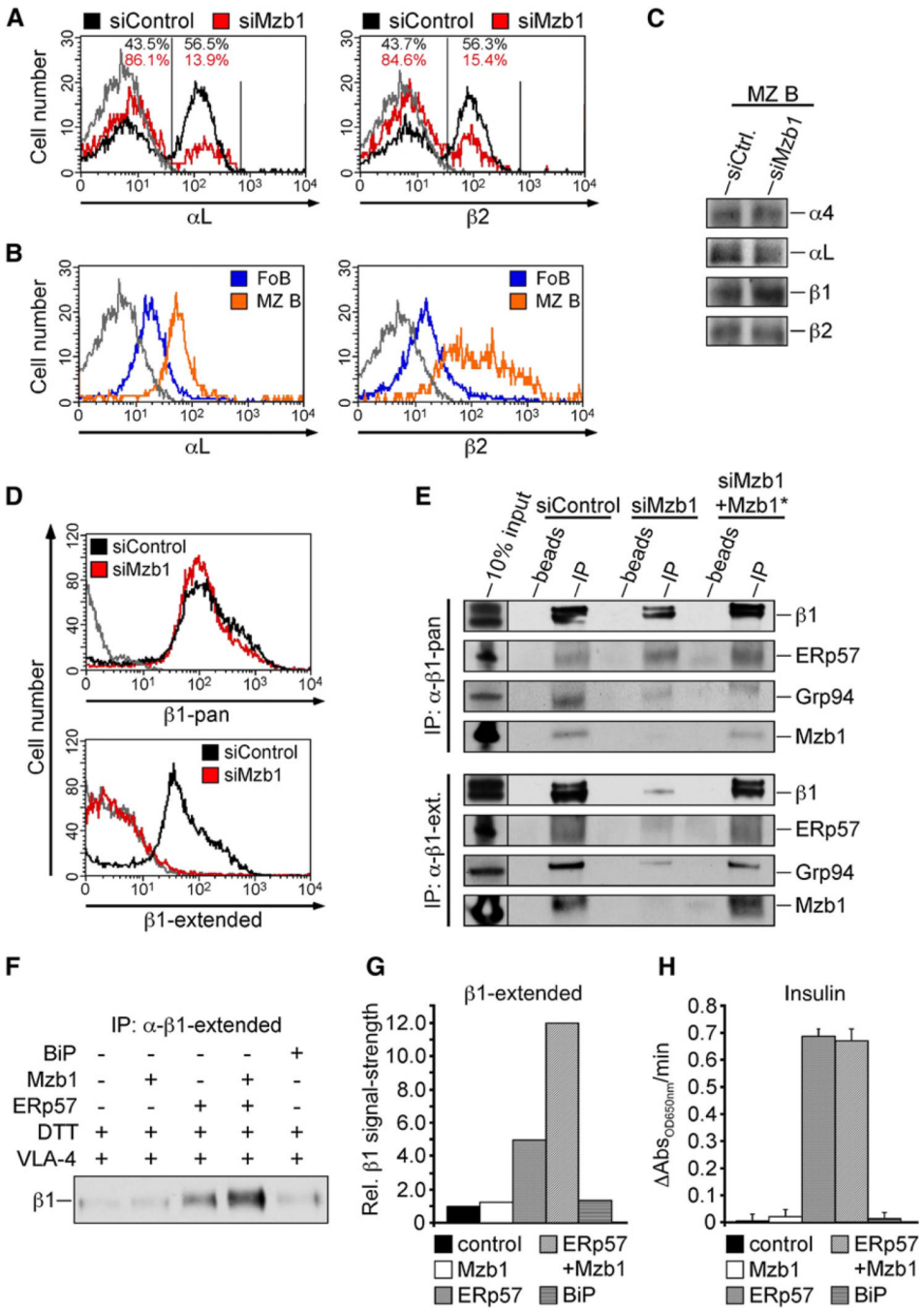

Figure 6. Mzb1 Regulates Integrin Folding by Substrate-Specific Enhancement of ERp57 Activity

(A and B) Flow cytometric analysis of αL and β2 surface integrin expression on (A) siControl- or siMzb1-MZ B cells and on (B) untreated FoB or MZ B cells. The solid gray line represents the isotype control, and FACS profiles reflect living or living and GFP-positive cells.

(C) Immunoblot analysis to detect expression of integrin chains in cell lysates of siControl- or siMzb1-MZ B cells.

(D) Flow cytometric analysis of surface integrin exression of either pan-β1 integrin or its extended form on siControl- or siMzb1-MZ B cells. FACS profiles reflect living, GFP-

positive cells, and data are representative of three independent experiments. The solid gray line represents the isotype control.

(E) Coimmunoprecipitation analysis of protein extracts from K46 cells expressing siControl, siMzb1, or siMzb1+Mzb1* using a pan-β1 integrin-specific or a β1 extended form-specific antibody for precipitation.

(F and G) Thiol-dependent catalytic activity of GST-ERp57, BiP, Mzb1 and GST-ERp57 combined with Mzb1 was measured using a VLA-4 folding assay. Human recombinant VLA-4 was incubated with the indicated proteins and the reduced and extended form of β1 integrin was immunoprecipitated. The precipitated protein was detected with a pan-β1 antibody. Densitometric analysis of the intensity of the β1 integrin-specific immunoblot signal, quantified by the AlphaEaseFC (AlphaImager 3400) software is presented in (G).

(H) Enzymatic activity of GST-ERp57, GST-BiP, Mzb1, and GST-ERp57 combined with Mzb1 was measured using the insulin turbidity assay. GST-BiP alone and an input sample lacking enzyme (control) are used as negative controls in this assay. $Absorbance_{OD650nm}$ values were collected and plotted as a function of time, and the enzymatic activity was calculated ($\Delta Abs_{OD650nm}$/min) (n = 3). Error bars indicate SD of the mean.

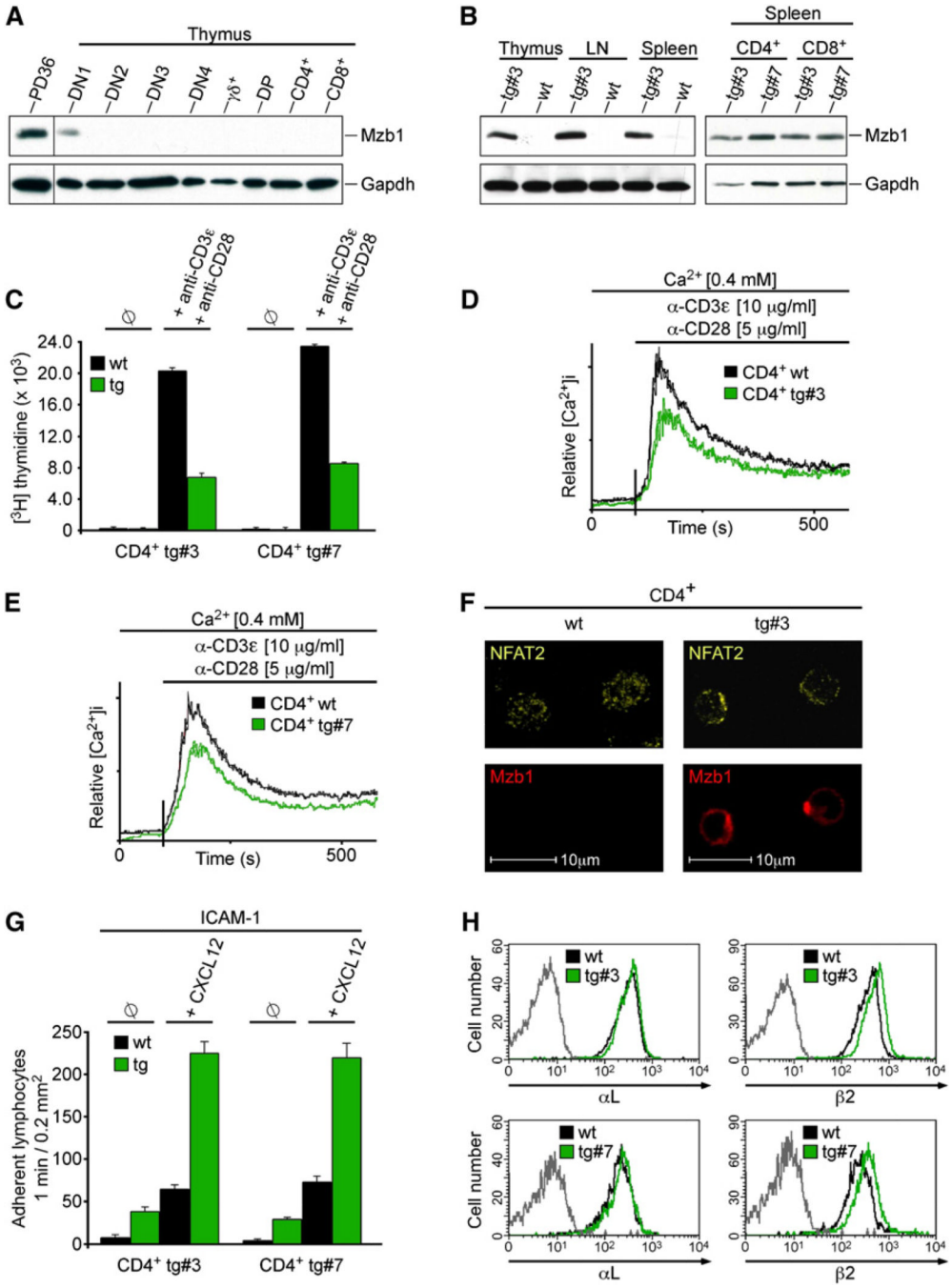

Figure 7. Ectopic Expression of Mzb1 in T Cells Alters Ca^{2+} Mobilization and Cell-Adhesion

(A) Immunoblot analysis to detect Mzb1 in protein extracts of FACS-sorted primary thymic T cell populations.

(B) Immunoblot analysis to detect Mzb1 in lysates from primary T cell populations derived from wild-type (wt) or *Lck-Mzb1* transgenic mice (lines #3 and #7).

(C) Analysis of cell proliferation of $CD4^+$ splenocytes from wild-type or *Lck-Mzb1* transgenic mice by determining [^{3}H] thymidine incorporation in cells without (ø) or with stimulation by anti-CD3ε (1 μg/ml) and anti-CD28 (1 μg/ml) for 16 hr. Data are expressed as the mean [^{3}H] thymidine incorporation of triplicate cultures and are representative of three independent experiments. Error bars indicate SD of the mean.

(D and E) Analysis of TCR-induced Ca^{2+} fluxes of $CD4^+$ splenocytes from wild-type or *Lck-Mzb1* transgenic mice (lines #3 and #7 shown in D and E, respectively) as described above. Data are representative of four independent experiments.

(F) Indirect immunofluorescence analysis of FACS-sorted and anti-CD3ε (10 μg/ml) plus anti-CD28 (5 μg/ml) stimulated wild-type or Mzb1-transgenic $CD4^+$ T cells (line #3) with anti-Mzb1 and anti-NFAT2 antibodies.

(G) Static adhesion assay to ICAM-1. Wild-type or Mzb1-transgenic $CD4^+$ T cells were treated with buffer (ø) or stimulated with CXCL12. Assays were performed in triplicate, and data are representative of three independent experiments. Error bars indicate SD of the mean.

(H) Flow cytometric analysis of αL and β2 surface integrin levels on wild-type or Mzb1-transgenic $CD4^+$ T cells (lines #3 and #7). The gray line represents the isotype control and data are representative of three independent experiments.